Monopole-Induced Emergent Electric Fields in Ferromagnetic Nanowires

Michalis Charilaou,[1,*] Hans-Benjamin Braun,[2,3,†] and Jörg F. Löffler[1]
[1]Laboratory of Metal Physics and Technology, Department of Materials, ETH Zurich, 8093 Zurich, Switzerland
[2]UCD School of Physics, University College Dublin, Dublin 04 V1W8, Ireland
[3]School of Theoretical Physics, Dublin Institute of Advanced Studies, Dublin 04 C932, Ireland

(Received 19 April 2018; published 28 August 2018; corrected 21 September 2018)

We predict that complete magnetization reversal in simple metallic ferromagnetic nanoparticles is directly linked to the pair creation of topological point defects in the form of hedgehog-antihedgehog pairs. These dynamical point defects move at exceptionally high speeds in excess of 1500 m/s, faster than any other known magnetic object. Their rapid motion generates unprecedented solenoidal emergent fields on the order of megavolts per meter, in analogy to the magnetic field of a moving electric charge, providing a striking example that a moving hedgehog constitutes an emergent magnetic monopole.

DOI: 10.1103/PhysRevLett.121.097202

The judicious ability to control magnetization reversal in nanostructures underpins the progress of magnetic technologies [1–3]. Magnetic switching may become surprisingly elaborate as dimensions become comparable to fundamental magnetic length scales even for nanoparticles that are in a single-domain state at remanence. Conventional wisdom associates magnetization reversal in cylindrical nanoparticles with curling-type processes [4,5], but these traditional considerations neglect the global topological constraints which preclude complete reversal via continuous processes.

So far, topological concepts have served to identify extraordinarily stable magnetization textures that play the role of controllable quasiparticles in the form of domain walls [6] or Skyrmions [7,8], which are considered as promising candidates for information carriers in prospective racetrack-type memories [6,7,9]. While static stabilization of Skyrmions requires materials with antisymmetric Dzyaloshinskii-Moriya interactions (DMI), topological arguments allow us to classify magnetization textures in completely general terms [10], as it is only topology which gives rise to emergent electromagnetic fields acting on the conduction electrons [11–13]. As topological stability implies the impossibility of continuous deformation into the uniform state, creation or decay of Skyrmions can only occur via the creation of topological point defects such as hedgehogs, Bloch points, or monopoles where the micromagnetic tenet [14] of a continuous magnetization field is violated [10,15–19].

In this Letter we show that such topologically nontrivial magnetization textures in the form of Skyrmions and hedgehogs play a central role in the magnetization reversal process in one of the most common and most widely studied nanoscale objects, namely a magnetic nanoparticle made of a simple metallic, DMI-free material. Such nanoparticles that are in a single-domain state at remanence [20,21] are highly relevant for spintronics [5,8,22], data storage [2], and biomedical applications [20,23].

We find that the irreversible magnetization switching behavior is linked to the nucleation and ultrafast linear motion of topological hedgehog defects that give rise to unprecedented forces on conduction electrons. These emergent electric fields are of the order of megavolts per meter and have solenoidal character, characterizing the moving hedgehogs as emergent magnetic monopoles. Specifically, based on high-resolution micromagnetic simulations, we find that in an elongated nanoparticle made of a simple ferromagnet, such as Permalloy or cobalt, the switching process that is initiated via the celebrated curling instability [20,21] proceeds in two stages: In the first stage, the instability develops into the formation of a Skyrmion line. This state is fully reversible, and hence upon removal of the applied field, the magnetization returns to its initial state. The second stage is irreversible and involves the breaking of the Skyrmion line with concomitant creation of singular topological point defects surrounded by 3D spin textures in the form of hedgehog-antihedgehog pairs, which after creation rapidly separate with velocities that significantly exceed those of domain walls [24], and which produce the strong emergent electric field.

The particles that we study are just beyond the Stoner-Wohlfarth regime, where the magnetization remains uniform at all times [25]. The particles are cylindrical and have a diameter comparable to $2\pi\delta_m$, with $\delta_m = 2(A/\mu_0 M_s^2)^{1/2}$, where A denotes the exchange stiffness and M_s the saturation magnetization. The simulations are based on the GPU-accelerated software package MuMax3 [26], which is based on a total energy density that includes ferromagnetic exchange, long-range dipolar interactions, single-ion anisotropy, and Zeeman coupling to an applied field $\mathbf{H}_{\text{ext}}$. The instantaneous magnetic state is characterized by the magnetization unit vector $\mathbf{m}(\mathbf{x}, t)$, which is

obtained by solving a discretized version of the Landau-Lifshitz-Gilbert (LLG) equation of motion $\partial_t \mathbf{m} = -\gamma\, \mathbf{m} \times \mathbf{H}_{\text{eff}} + \alpha\, \mathbf{m} \times \partial_t \mathbf{m}$. Here α is the dimensionless damping parameter, γ is the electron gyromagnetic ratio, and the effective field acting on the local magnetization is defined as the functional derivative of the total energy E with respect to the magnetization, $\mu_0 \mathbf{H}_{\text{eff}} = -(1/M_s)\delta E/\delta \mathbf{m}$.

The simulations presented here are for Permalloy ($Fe_{20}Ni_{80}$) with exchange stiffness $A = 13$ pJ/m and saturation magnetization $M_s = 800$ kA/m. We chose this material because it is commonly synthesized in laboratories in the form of nanoparticles and nanowires, which makes the experimental realization of our predictions highly feasible. For most simulations, we considered the high-damping case with $\alpha = 0.1$. Occasional checks with $\alpha = 0.01$ and 0.001 were made to test the effects of damping on the simulation findings, but no significant change in the results was found. Apart from Permalloy, we also considered a wide range of materials with different values of the magnetocrystalline uniaxial anisotropy K_u and found that the phenomena presented are valid as long as $2K_u/\mu_0 M_s^2 < 1$; i.e., when the magnetocrystalline anisotropy is smaller than the shape anisotropy of the wire (see Fig. 1 of the Supplemental Material in Ref. [27]), and when the diameter of the cylinder is comparable to $\pi\delta_m$.

The nanowires studied in this paper have a diameter of 60 nm and a length of 300 nm. The cell size is set to 1.87 nm × 1.87 nm × 2.35 nm. Smaller and larger cell sizes were also implemented to verify the numerical stability of the results, with the cell size never being larger than $\delta_m/2 = (A/\mu_0 M_s^2)^{1/2} \approx 4$ nm or smaller than 1 nm. Even though small cell sizes were used, quantum effects were not considered in our simulations.

In a cylindrical nanowire of Permalloy, with a high aspect ratio (in this example 5:1), the equilibrium magnetization nearly equals the saturation value, only slightly reduced due to dipolar-induced curling at the ends of the cylinder [cf. Fig. 1(a)]. Note that the sense of curling is arbitrary and constitutes spontaneous symmetry breaking. Once a constant external field is applied opposing the remanent state, the reversal emanates from the two ends as the spin texture "curls" around the cylinder. With increasing field strength and duration, such curling becomes more pronounced when two domains with opposite chirality propagate towards the middle of the cylinder to reduce the dipolar energy of the system [cf. Figs. 1(b)–1(e)]. As time progresses, the spins on the outer rim of the wire align with the external field, whereas spins in the center point along the original remanent direction. The z component of the magnetization of this state fits that of a 2π-domain wall profile [see Fig. 1(d)] consisting of a soliton pair [10,28]: $\pi - \theta = \theta_s(\rho/\delta + R) + \theta_s(\rho/\delta - R)$, with $\theta_s(\xi) = 2\arctan e^{-\xi}$ being the polar angle of a π-domain wall. Here ρ denotes the distance from the center, δ the intrinsic length scale, and R a variational parameter. Together with the azimuthal angle ϕ, the polar angle θ parametrizes the magnetization unit vector via $\mathbf{m} = (\sin\theta\cos\phi, \sin\theta\sin\phi, \cos\theta)$. In Fig. 1(e), the azimuthal angle ϕ describes a Bloch wall configuration, and the resulting texture in Figs. 1(b) and 1(c) is a topologically nontrivial object, namely a *Skyrmion line* [29], reflected by a nonzero, integer topological charge evaluated across a cross section D of the wire. As we also

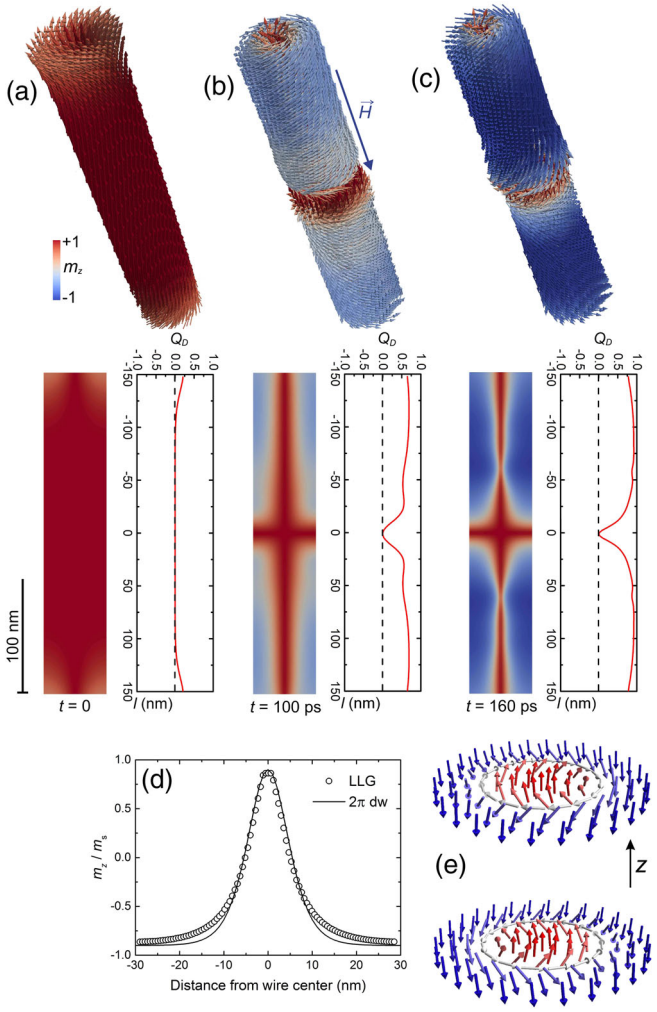

FIG. 1. Snapshots of a micromagnetic simulation showing the initial, reversible stages of the switching process in a cylindrical Permalloy nanowire with diameter 60 nm and length 300 nm: (a) at 0 s, (b) at 100 ps, and (c) at 160 ps, after having applied a constant field of 125 mT along $-z$. The top panels show vector-field plots, and the bottom panels show contour plots of the z component of the magnetization together with the topological charge density integrated across the cylinder. The initial curling-mode instability develops into the formation of two Skyrmion lines of opposite handedness. The graph in (d) shows the profile across the wire taken 100 nm from its middle, well described by the variational ansatz discussed in the text, and (e) schematically indicates the Skyrmion spin textures of opposite chirality that are obtained in (b) and (c) at sample cross sections at $\pm z_0$, with $z_0 \approx 50$–150 nm.

wish to describe hedgehog-like point defects, we write the topological charge in completely general form [10]:

$$Q_{\mathcal{M}} = \frac{1}{4\pi}\int_M \epsilon_{abc} m^a dm^b \wedge dm^c = \frac{1}{4\pi}\int dudv\mathcal{J}\sin\theta, \tag{1}$$

where $\mathcal{J} = \partial_u\theta\partial_v\phi - \partial_v\theta\partial_u\phi$. Here the curvilinear coordinates u, v parametrize the 2D manifold $\mathcal{M}$, which is either a disk D for a Skyrmion, or a sphere S^2 around a topological point defect surrounded by a 3D spin texture, such as the hedgehog discussed below. Correspondingly, Q_D and Q_{S^2} denote the respective winding numbers. As shown in Fig. 1(c), $Q_D \approx 1$ nearly everywhere along the wire except at the wire ends due to the twisting of the moments on the surface. The two Skyrmion lines have opposite chirality [see Fig. 1(c)], thus repelling each other, which establishes a nearly uniform state with $Q_D \approx 0$ in the central region that shrinks only gradually with increasing field duration and strength (see Fig. 1).

At the critical value of the external magnetic field, the dynamics exhibits critical slowing down, and switching will occur only after an infinitely long field exposure (cf. Fig. 2 of the Supplemental Material in Ref. [27]). For supercritical fields there is no energy barrier, and the switching process depends crucially on the duration of the applied field. As shown in Fig. 2, if the field is switched off before the Skyrmion lines break, the process is fully reversible, and no magnetization switching occurs. In fact, the magnetization returns to its original remanent state within a fraction of a nanosecond, reminiscent of a radial exchange spring; see video 1 in the Supplemental Material [27]. Importantly, the state shown in Fig. 2(a) does not contain any point defects; i.e., $Q_{S^2} = 0$ everywhere. Irreversible magnetization switching only occurs if the field is applied long enough to break the Skyrmion lines, which entails the pair creation of point defects [see Fig. 2(b)]. Such pair creation abruptly introduces singular topological defects in the form of hedgehogs, or Bloch points, as shown in Fig. 3(e), which are characterized by $Q_{S^2} = \pm 1$. Hence, we find that the existence of a nonzero topological point charge $Q_{S^2} \neq 0$ is a direct measure of the irreversibility of the magnetization process, while the process remains reversible as long as $Q_{S^2} = 0$ everywhere. Note that the pair creation of point defects is a purely dynamical effect, unlike the static point defects at the ends of broken Skyrmion lines [15] or chiral bobbers [30,31] in DMI materials.

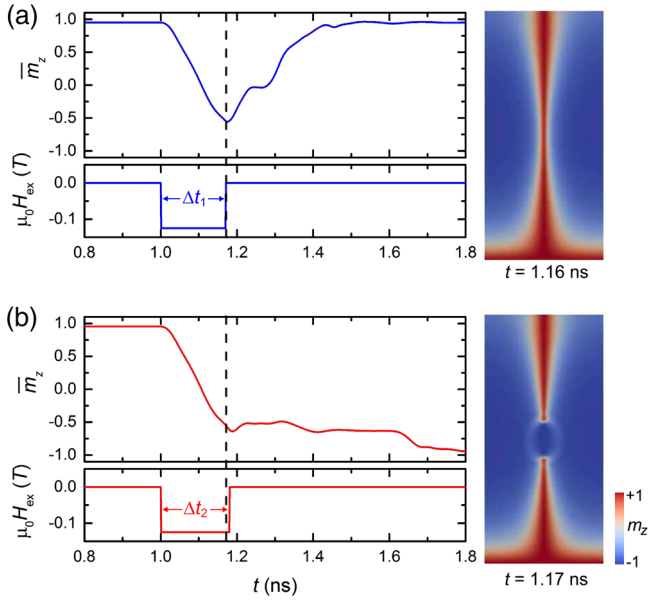

FIG. 2. Time evolution of the spatially averaged magnetization $\bar{m}_z$ during a field pulse, and contour plot of m_z10 ps before the applied magnetic field is switched off: (a) The magnetization process is reversible if the applied field is switched off before the Skyrmion lines break ($\Delta t_1 = 0.16$ ns). (b) Irreversibility sets in only when the Skyrmion line is destroyed via the creation of a hedgehog-antihedgehog pair before switching off the applied field ($\Delta t_2 = 0.17$ ns). Only in the latter case does full magnetization reversal occur ($\bar{m}_z \approx -1$).

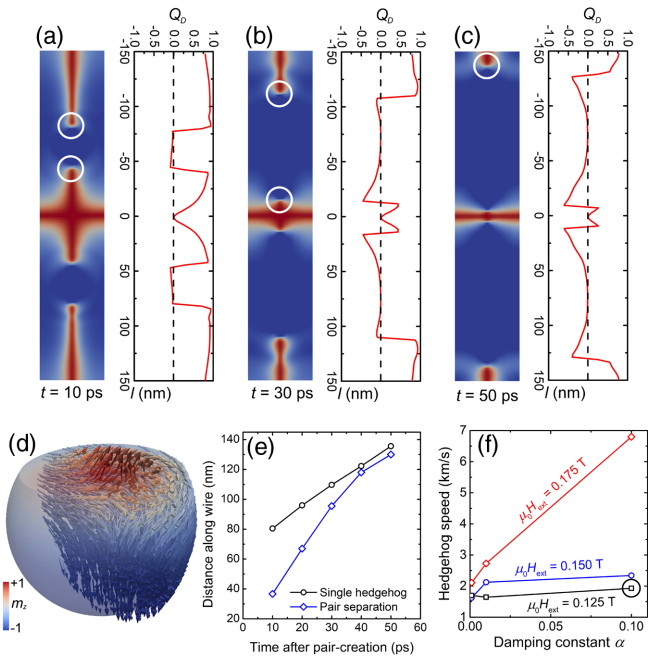

FIG. 3. Contour plots of m_z and Q_D as a function of z at (a) $t = 10$ ps, (b) $t = 30$ ps, and (c) $t = 50$ ps after the field has been switched off. The circles in the contour plots indicate the positions of the $Q_{S^2} = 1$ (top) hedgehog and the $Q_{S^2} = -1$ (bottom) antihedgehog as a function of time. (d) Detailed view of the moment distribution of a hedgehog at the end of the Skyrmion line. (e) Hedgehog separation (diamonds) and location of the top hedgehog (circles) as a function of time, yielding a maximal relative velocity of $\approx 3 \times 10^3$m/s. (f) Hedgehog speed as a function of the damping constant α at three different external fields. In panels (a)-(e) the values $\alpha = 0.1$ and $\mu_0 H_{\text{ext}} = 0.125$ T were used, as marked with a circle in panel (f).

This change of topology generates a new dynamical state of magnetic matter in the nanowire. The hedgehogs rapidly move away from each other, as seen in Figs. 3(a)–3(c), which show their separation as a function of time. In fact, the relative velocity of the hedgehogs is ∼3000 m/s [cf. Fig. 3(d) (for an external field of 0.125 T)], higher than any fast-moving topological textures known so far [24]. The velocity depends on the damping constant and the effective magnetic field in the material. Specifically, the hedgehogs become increasingly fast with increasing external field, and the velocity can reach values as high as 6–7 km/s [see Fig. 3(f)].

Importantly, the movement of the hedgehogs along the wire produces an *emergent electric field*, as illustrated in Fig. 4. Moving topologically nontrivial spin textures have been thought to give rise to only weak emergent electric fields that act on the conduction electrons. However, this conclusion has been reached on the basis of materials exhibiting DMI [15–17,32]. In contrast, we consider materials that are simple ferromagnets. The formation of the Skyrmion lines, and consequently of the hedgehogs, is thus a dynamic effect produced solely from the topology of the magnetic spin texture in the cylindrical nanowires. Further, the ultrafast movement of the hedgehogs in a straight line has to our knowledge never been observed, and it has striking consequences: the emergent electric field due to the hedgehog's linear movement has solenoidal character, in analogy to the magnetic field of a moving electric charge; the components of the emergent electric field are given by $E_i^{\mathrm{em}} = \hbar \mathbf{m} \cdot (\partial_i \mathbf{m} \times \partial_t \mathbf{m})$ [11,12]. For electrons aligned with magnetization parallel to the magnetization unit vector $\mathbf{m}$ (i.e., spin antiparallel to $\mathbf{m}$), the emergent electric charge is given by [12] $q_{\downarrow}^{\mathrm{em}} = -1/2$, and for the opposite spin $q_{\uparrow}^{\mathrm{em}} = +1/2$. Thus, the net force on a conduction electron due to the emergent E field is given by $\mathbf{F} = q^{\mathrm{em}}\mathbf{E}^{\mathrm{em}}$. For the spin texture of a vertically moving hedgehog, as shown in Fig. 3, the emergent field $\mathbf{E}^{\mathrm{em}}$ has a solenoidal character as shown in Fig. 4, and the magnitude of the force is given by $F \approx \hbar v/2\lambda^2$. Here λ is the characteristic length of the Bloch-point spin texture, and v is its velocity. For the values obtained from our simulations ($v \approx 1500$ m/s and $\lambda \approx \delta \approx 1$ nm), we obtain $F \approx 7.87 \times 10^{-14}$ J/m, which corresponds to the force exerted on an electron by a real electric field with magnitude $E_{\mathrm{real}} \approx 0.5$ MV/m. This value is strikingly large, and it is within an order of magnitude of the dielectric breakdown in vacuum (∼3 MV/m), solely produced by a single moving hedgehog. As noted above, considering that the hedgehog speed increases with increasing external field, even stronger emergent fields are possible. Importantly, this result provides a striking example that the moving hedgehog constitutes an emergent magnetic monopole.

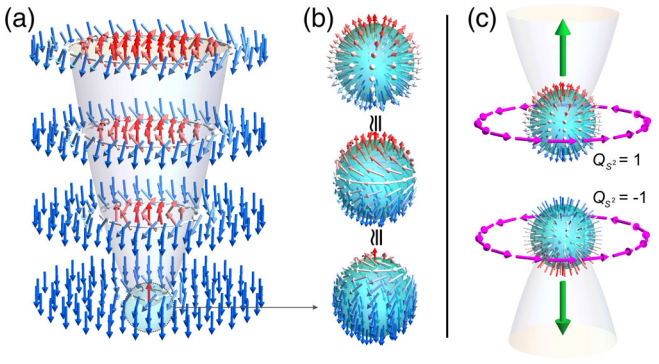

FIG. 4. (a) Schematic view of the end of a Skyrmion line, where (b) the corresponding magnetization texture is seen to be topologically equivalent to a hedgehog with radially outward-oriented magnetization ($Q_{S^2} = 1$). (c) A pair of separating hedgehogs of opposite topological charge ($Q_{S^2} = \pm 1$) gives rise to an emergent solenoidal electric field (purple), in analogy to the magnetic field created by a pair of separating electric charges of opposite sign. For the process shown in Fig. 3, the emergent electric field of such a magnetic monopole has a strength of the order of 0.5 MV/m.

Note that the monopoles moving towards the ends of the wire are absorbed by the surfaces, whereas the monopoles moving towards the middle of the wire oscillate axially before they are annihilated; see video 2 in the Supplemental Material [27]. These oscillations have a time constant on the order of 10 ps and hence generate emergent electric fields with frequencies in the terahertz range. This in turn suggests that upon switching, ferromagnetic nanowires, or simply nanoparticles with uniaxial anisotropy, may emit measurable radiation due to the accelerating electrons, and we propose that this could be detected in pump-probe switching experiments.

After the hedgehogs have been absorbed, the wire is in a 3-domain state with a 2π-domain wall. Eventually the latter is annihilated via *escape through the third dimension* [28] into a collinear state, thus resulting in a single-domain state pointing along the external field.

Note that even for other material shapes, such as ellipsoids or cuboids with uniaxial symmetry, and even in the presence of surface anisotropy, the phenomena described above persist with monopole motion accompanied by an emergent electric field (cf. Fig. 3 of the Supplemental Material in Ref. [27]), as long as curling is not suppressed. Further, we have also considered nanowires at finite temperature and found that these phenomena remain valid even in the presence of thermal fluctuations (cf. Fig. 4 of the Supplemental Material in Ref. [27]). This opens new possibilities for fundamental investigations into the dynamics of topological point defects in nanostructures and for the development of advanced devices exploiting the physics of emergent fields, all based on simple metallic ferromagnets without DMI.

In conclusion, we have found that magnetization switching in ferromagnetic nanoparticles is directly linked to the formation and dynamics of topological point defects. In the

example shown here, the switching occurs via the formation of two Skyrmion lines. As long as the Skyrmion lines are intact, the switching is fully reversible upon switching off the external magnetic field. As soon as the Skyrmion lines break, however, hedgehog-antihedgehog pairs are created, and the switching becomes irreversible. The rapidly moving hedgehogs generate an emergent electric field with substantially high magnitude and a solenoidal character, thus characterizing them as emergent magnetic monopoles. Hence, nontrivial topological spin textures and magnetic monopoles plus their dynamics play a key role in the switching process of magnetic nanoparticles. Based on this, we have found a way to precisely generate and control topological defects in nanoscale ferromagnets, which may enable a technology that exploits emergent electromagnetic fields in the terahertz range.

M. C. and J. F. L. gratefully acknowledge funding from the ETH Research Grant No. ETH-47 17-1, and H.-B. B. thanks the Science Foundation of Ireland (Grant No. 11-PI-1048). H. B. B. would like to thank W. Nahm for insightful discussions.

*charilaou@mat.ethz.ch
Present address: Department of Physics, University of Louisiana at Lafayette, Lafayette, Louisiana 70504, USA. michalis.charilaou@louisiana.edu
†bbraun@stp.dias.ie

[1] S. Parkin and S.-H. Yang, Nat. Nanotechnol. **10**, 195 (2015).
[2] S. Sun, C. B. Murray, D. Weller, L. Folks, and A. Moser, Science **287**, 1989 (2000).
[3] D. Sander, S. O. Valenzuela, D. Makarov, C. H. Marrows, E. E. Fullerton, P. Fischer, J. McCord, P. Vavassori, S. M. P. Pirro, B. Hillebrands, A. D. Kent, T. Jungwirth, O. Gutfleisch, C. G. Kim, and A. Berger, J. Phys. D **50**, 363001 (2017).
[4] A. Aharoni, *Introduction to the Theory of Ferromagnetism* (Clarendon Press, Oxford, England, 2000).
[5] A. Fernández-Pacheco, R. Streubel, O. Fruchart, R. Hertel, P. Fischer, and R. P. Cowburn, Nat. Commun. **8**, 15756 (2017).
[6] S. S. P. Parkin, M. Hayashi, and L. Thomas, Science **320**, 190 (2008).
[7] J. Sampaio, V. Cros, S. Rohart, A. Thiaville, and A. Fert, Nat. Nanotechnol. **8**, 839 (2013).
[8] W. Jiang, G. Chen, K. Liu, J. Zang, S. G. te Velthuis, and A. Hoffmann, Phys. Rep. **704**, 1 (2017).
[9] S. Woo, K. Litzius, B. Krüger, M.-Y. Im, L. Caretta, K. Richter, M. Mann, A. Krone, R. M. Reeve, M. Weigand, P. Agrawal, I. Lemesh, M.-A. Mawass, P. Fischer, M. Kläui, and G. S. D. Beach, Nat. Mater. **15**, 501 (2016).
[10] H.-B. Braun, Adv. Phys. **61**, 1 (2012).
[11] G. E. Volovik, J. Phys. C **20**, L83 (1987).
[12] T. Schulz, R. Ritz, A. Bauer, M. Halder, M.Wagner, C. Franz, C. Pfleiderer, K. Everschor, M. Garst, and A. Rosch, Nat. Phys. **8**, 301 (2012).
[13] Y. Tokura, M. Kawasaki, and N. Nagaosa, Nat. Phys. **13**, 1056 (2017).
[14] W. Brown, *Micromagnetics* (Interscience Publishers, New York, 1963).
[15] P. Milde, D. Köhler, J. Seidel, L. M. Eng, A. Bauer, A. Chacon, J. Kindervater, S. Mühlbauer, C. Pfleiderer, S. Buhrandt, C. Schütte, and A. Rosch, Science **340**, 1076 (2013).
[16] C. Schütte and A. Rosch, Phys. Rev. B **90**, 174432 (2014).
[17] N. Kanazawa, Y. Nii, X.-X. Zhang, A. Mishchenko, G. De Filippis, F. Kagawa, Y. Iwasa, N. Nagaosa, and Y. Tokura, Nat. Commun. **7**, 11622 (2016).
[18] R. Hertel, J. Phys. Condens. Matter **28**, 483002 (2016).
[19] M. Charilaou and J. F. Löffler, Phys. Rev. B **95**, 024409 (2017).
[20] K. M. Krishnan, *Fundamentals and Applications of Magnetic Materials* (Oxford University Press, Oxford, England, 2016).
[21] A. P. Guimaraes, *Principles of Nanomagnetism* (Springer, New York, 2017).
[22] P. Bruno, V. K. Dugaev, and M. Taillefumier, Phys. Rev. Lett. **93**, 096806 (2004).
[23] E. Myrovali, N. Maniotis, A. Makridis, A. Terzopoulou, V. Ntomprougkidis, K. Simeonidis, D. Sakellari, O. Kalogirou, T. Samaras, R. Salikhov, M. Spasova, M. Farle, U. Wiedwald, and M. Angelakeris, Sci. Rep. **6**, 37934 (2016).
[24] S.-H. Yang, K.-S. Ryu, and S. Parkin, Nat. Nanotechnol. **10**, 221 (2015).
[25] W. Wernsdorfer, Adv. Chem. Phys. **118**, 99 (2001).
[26] A. Vansteenkiste, J. Leliaert, M. Dvornik, M. Helsen, F. Garcia-Sanchez, and B. V. Waeyenberge, AIP Adv. **4**, 107133 (2014).
[27] See Supplemental Material at http://link.aps.org/supplemental/10.1103/PhysRevLett.121.097202 for an analysis of critical slowing down, anisotropy, particle morphology, and finite-temperature effects.
[28] H.-B. Braun, Phys. Rev. B **50**, 16485 (1994).
[29] H.-B. Braun, J. Appl. Phys. **85**, 6172 (1999).
[30] F. Zheng, F. N. Rybakov, A. B. Borisov, D. Song, S. Wang, Z.-A. Li, H. Du, N. S. Kiselev, J. Caron, A. Kovács, M. Tian, Y. Zhang, S. Blügel, and R. E. Dunin-Borkowski, Nat. Nanotechnol. **13**, 451 (2018).
[31] A. S. Ahmed, J. Rowland, B. D. Esser, S. R. Dunsiger, D. W. McComb, M. Randeria, and R. K. Kawakami, Phys. Rev. Mater. **2**, 041401 (2018).
[32] S.-Z. Lin and A. Saxena, Phys. Rev. B **93**, 060401(R) (2016).

Correction: The first byline footnote has been restructured for clarity.